pH-Responsive Diblock Copolymers Prepared by the Dual Initiator Strategy

Katrien V. Bernaerts,[†] Nicolas Willet,[‡] Wim Van Camp,[†] Robert Jérôme,[‡] and Filip E. Du Prez*,[†]

Department of Organic Chemistry, Polymer Chemistry Research Group, Ghent University, Krijgslaan 281 (S4-bis), 9000 Ghent, Belgium, and Center for Education and Research on Macromolecules (CERM), University of Liège, Sart-Tilman B6a, B-4000 Liège, Belgium

Received December 8, 2005; Revised Manuscript Received March 20, 2006

ABSTRACT: Diblock copolymers poly(tetrahydrofuran-*b*-*tert*-butyl acrylate) (PTHF-*b*-PtBA) and poly(tetrahydrofuran-*b*-1-ethoxyethyl acrylate) (PTHF-*b*-PEEA) were successfully synthesized by the dual initiator 4-hydroxybutyl-2-bromoisobutyrate (HBBIB). The isobutyrate and alcohol function of HBBIB were used for the atom transfer radical polymerization of tBA (or EEA) and the living cationic ring-opening polymerization of THF, respectively. Hydrolysis or thermolysis of the aforementioned diblock copolymers results in amphiphilic pH-responsive copolymers PTHF-*b*-poly(acrylic acid) (PTHF-*b*-PAA). Matrix-assisted laser desorption/ionization time-of-flight (MALDI-TOF) and nuclear magnetic resonance spectroscopy (^{1}H NMR) were used to analyze the PTHF macroinitiator, while clear evidence for the formation of well-defined block copolymer structures was obtained by ^{1}H NMR, gel permeation chromatography (GPC), and infrared spectroscopy (FT-IR). The amorphous PtBA block in PTHF-*b*-PtBA resulted in a decrease of the crystallinity and the melting point of PTHF, as shown by differential scanning calorimetry (DSC). Self-assembly of PTHF-*b*-PAA copolymers in water into aggregates and micelles when exposed to specific pH values was confirmed by dynamic light scattering, infrared, and NMR spectroscopies.

Introduction

Intelligent, responsive polymers are receiving steadily increasing attention as a result of their ability to change drastically their physical state under small changes of external parameters, such as temperature,[1] pH,[2] light illumination, or electric or magnetic fields. Stimuli-sensitive amphiphilic block copolymers are a well-known class of intelligent polymers with a variety of promising potential applications, e.g., entrapment of environmental pollutants,[3] catalysis,[4] stabilizers in emulsion polymerization,[5] drug carriers,[6] nanoreactors,[7] and polymeric surfactants.[1,8]

There is a need for novel well-defined and "tailor-made" block copolymers in order to broaden the range of their properties and applications. Living polymerization techniques are a prerequisite for their successful synthesis. However, each technique is effective for only a limited range of monomers, which limits the diversity of accessible block copolymers. The range of possible monomer combinations in block copolymers is greatly extended when the polymerization mechanism is changed to suit the reactivity of the monomers to be polymerized sequentially.[9] More recently, the use of dual initiators has been proposed as an alternative strategy.[10−22] Dual initiators contain two initiating agents, each of them being selective for monomers polymerized by a given polymerization mechanism, in such a way that this initiator is attached to each type of growing chains.

In this paper, the dual initiator strategy has been used to prepare pH-responsive block copolymers based on poly(tetrahydrofuran) (PTHF) and poly(acrylic acid) (PAA) by combining cationic ring-opening polymerization (CROP) and atom transfer radical polymerization (ATRP). The OH function of the dual initiator 4-hydroxybutyl-2-bromoisobutyrate (HBBIB) can initiate CROP of THF, as reported elsewhere.[21] The bromoisobutyrate end group serves as an ATRP initiator for the polymerization of *tert*-butyl acrylate (tBA) and 1-ethoxyethyl acrylate (EEA), which are a protected version of acrylic acid.[23] The acrylic acid group can be regenerated by hydrolysis of PtBA and thermolysis of PEEA, respectively. Therefore, novel amphiphilic pH-responsive block copolymers have been synthesized that contain a hydrophobic PTHF block and a hydrophilic pH-responsive PAA block. This type of diblock copolymer self-assembles into micelles when exposed to water at specific pH's.[24−26]

The hydrophobic interactions of the nonionic blocks result in a micellar core that is surrounded by a charged corona of the ionic blocks.[27] Most of the work on ionic amphiphilic block copolymers refers to diblock copolymers with a polystyrene hydrophobic block and a poly(methacrylic acid) (PMAA)[4,28−33] or PAA[34−37] ionic block. Because of the relatively high glass transition temperature of polystyrene (T_g = 100 °C), these diblock copolymers are dissolved in water either by heating for sufficient long time slightly below 100 °C or by stepwise dialysis from an organic solvent common to the two blocks and miscible with water (e.g., tetrahydrofuran, dioxane, dimethylformamide). Because these techniques are time-consuming, attention is paid now to hydrophobic blocks with a low T_g, such as poly(butyl acrylate)[38] ($T_g \approx -52$ °C), poly(ethyl acrylate) ($T_g \approx -31$ °C),[39] poly(isobutylene)[40,41] ($T_g \approx -65$ °C) and, in this work, PTHF ($T_g \approx -86$ °C). Dissolution in water is not only much easier, but the mobility and permeability of the core are increased.[38,39]

We investigated the micellization of the ionic amphiphilic diblock copolymers, PTHF-*b*-PAA, with PTHF of a constant degree of polymerization (DP_{PTHF} = 68) and PAA of different DP's by dynamic light scattering (DLS), Fourier transform infrared spectroscopy (FT-IR), and nuclear magnetic resonance spectroscopy (NMR). The effect of the amorphous PtBA block

[†] Ghent University.
[‡] University of Liège.
* Corresponding author: Tel +32 9264 45 03; Fax +32 9264 49 72; e-mail Filip.Duprez@UGent.be.

10.1021/ma052625t CCC: $33.50
Published on Web 04/22/2006

on the crystallinity of PTHF has also been studied by differential scanning calorimetry (DSC).

Experimental Section

Materials. tBA (Fluka, 98+%) was purified by vacuum distillation (60 °C/60 mmHg). Inhibitor was removed from styrene (Acros, 99%) by passing it through basic alumina. EEA was synthesized as described previously.[23] CuBr (Aldrich, 98%) was purified by stirring with acetic acid. After filtration, it was washed with methanol and ether and then dried under vacuum at 70 °C. *N*,*N*,*N*′,*N*″,*N*″-Pentamethyldiethylenetriamine (PMDETA, Acros, 99+%) was distilled (85−86 °C/12 mmHg). Trifluoromethanesulfonic anhydride (Tf_2O, Acros, 98+%) was purified by distillation under atmospheric pressure (81−83 °C). Dichloromethane was extracted three times with pure sulfuric acid and washed three times with a concentrated aqueous sodium hydroxide (10% w/v). Then, it was washed several times with distilled water until the pH became neutral. The purified dichloromethane was dried for several hours on magnesium sulfate, filtered off, and then refluxed for 2 h over calcium hydride. Dichloromethane was distilled, stored over calcium hydride, and refluxed over calcium hydride prior to use. Allyl alcohol (AllylOH, Aldrich, >98.5%) was purified by distillation at 96−98 °C. 2,2,6,6-Tetramethylpiperidine (TMP, Acros, 98%) was purified by distillation at 152 °C under a nitrogen atmosphere. Tetrahydrofuran (Acros, 99.8%) was distilled from CaH_2 and used after distillation over sodium in the presence of benzophenone. 2,6-Di-*tert*-butylpyridine (DTBP, Maybridge Chemicals, 97+%) and trifluoroacetic acid (TFA, Acros, 99%) were used as received. 4-Hydroxybutyl-2-bromoisobutyrate (HBBIB) was prepared as described earlier.[21] (Trimethylsilyl)diazomethane (2 M solution in hexane) was supplied by Aldrich and used as received.

Preparation of PTHF-Br by the CROP of THF with HBBIB/Tf_2O/DTBP. A typical procedure for the two-stage polymerization of THF is as follows (see $PTHF_{68}$ in Table 1). In a flame-dried two-necked flask of 250 mL, CH_2Cl_2 (28 mL), DTBP (2.00 mL, 8.92 mmol), and Tf_2O (1.00 mL, 5.94 mmol) were placed at 0 °C under a nitrogen atmosphere. To this solution HBBIB (1.66 g, 6.95 mmol) was added under vigorous stirring, and the mixture was stirred for 1 h at 0 °C. The initiator solution was brought to 25 °C, after which an initial amount of 8.0 mL THF (99 mmol) was introduced. After 2 h, the main amount of THF (72 mL, 0.89 mol) was added. The polymerization was carried out at 25 °C for the prescribed reaction time (21 min for $PTHF_{68}$ in Table 1, 15% conversion) and was terminated quantitatively with 4 equiv of allyl alcohol relative to the growing chains (1.63 mL, 23.8 mmol), using TMP (4.0 mL, 24 mmol) as a proton trap. The resulting TMP salt was filtered off, and the reaction mixture was evaporated. The polymer was dissolved in CH_2Cl_2 and extracted three times with cold basic water (1 M KOH). After drying of the collected organic layers with $MgSO_4$ and after evaporation of the solvent, the polymer was finally redissolved in a minimal amount of THF and precipitated in cold pentane. The white powder was filtered off, washed with cold pentane, and dried under vacuum. The allyl and Br functionality of PTHF was confirmed by ^{1}H NMR, MALDI-TOF (Figure 1), and FT-IR.

^{1}H NMR (300 MHz, $CDCl_3$) δ (ppm): 1.60 (4H, $-CH_2CH_2-$ protons of PTHF), 1.92 (s, 6H, $-C(CH_3)_2-$), 3.41 (4H, $-OCH_2-$ protons of PTHF), 3.97 (doublet of doublets, 2H, $-OCH_2CH=CH_2$), 4.19 (t, 2H, $-CH_2O(C=O)-$), 5.14 (doublet of quartets, 1H, $-OCH_2CH=CH_2$), 5.28 (doublet of quartets, 1H, $-OCH_2CH=CH_2$), 5.92 (m, 1H, $-OCH_2CH=CH_2$)

FT-IR (KBr, CH_2Cl_2) ν (cm^{-1}): 3035−2799 (s), 1731 (w) (ester initiator), 1645 (w) (ν C=C), 1484−1422 (m), 1370 (m) (PTHF), 1200−1284 (w), 1106 (vs) (υ_{as} C−O−C PTHF)

Preparation of PTHF-*b*-PtBA by ATRP with PTHF-Br as Macroinitiator. In a typical polymerization (see $PTHF_{68}$-*b*-$PtBA_{12}$ in Table 2), the PTHF macroinitiator (2.31 g, 0.436 mmol), tBA monomer (9.5 mL, 0.065 mol), PMDETA (0.091 mL, 0.44 mmol) and acetone (33 vol %) were added to a flask equipped with a reflux condenser. The reaction mixture was degassed by three freeze−pump−thaw cycles. CuBr (0.0626 g, 0.436 mmol) was added to the frozen reaction mixture under a nitrogen atmosphere. The flask was closed and evacuated by three nitrogen/vacuum cycles. The flask was then immersed in an oil bath thermostated at 75 °C. Samples were withdrawn periodically to monitor monomer conversion (by ^{1}H NMR) and molecular weight (by gel permeation chromatography, GPC). After a certain reaction time (50 min, 13% conversion for $PTHF_{68}$-*b*-$PtBA_{12}$), the polymerization was terminated in liquid nitrogen. Block copolymers were dissolved in THF, purified by passing through neutral alumina, and precipitated in cold pentane (low content of PtBA) or in a 50/50 MeOH/water mixture (high PtBA content). The initiation efficiency of the PTHF-Br macroinitiator was very high, as no residual macroinitiator could be observed in GPC after block copolymerization. Typical GPC traces are shown in Figure 3a,c and Figure 5a,b.

^{1}H NMR ($CDCl_3$, 500 MHz) δ (ppm): 1.12 (s, 6H, $-C(CH_3)_2-$), 1.18−2.02 (broad, 15H, $CH_2/C(CH_3)_3$ protons of PtBA and $-CH_2CH_2-$ protons of PTHF), 2.22 (s, 1H, C*H*− protons of PtBA), 3.41 (4H, $-OCH_2-$ protons of PTHF), 3.95 (d of t, 2H, $CH_2=CHCH_2-$), 4.04 (m, 3H, R_2CHBr and $-CH_2OC(=O)-$), 5.17 and 5.28 (d of quartets, 2H, $CH_2=CH-$), 5.90 (m, 1H, $CH_2=CH-$).

FT-IR (KBr, CH_2Cl_2) ν (cm^{-1}): 3054, 2984, 2941, 2867 (s), 1725 (vs) (C=O, ester), 1605 (w) ($\nu_{C=C}$), 1551 (w), 1478 (m), 1446 (m), 1422 (m), 1393 and 1368 (tBu), 1265 and 1152 (s) (υ_{as} C−O−C), 1107 (m), 896 (m), 734 (m).

Preparation of PTHF-*b*-PEEA by ATRP with PTHF-Br as Macroinitiator. A typical polymerization procedure is as follows ($PTHF_{68}$-*b*-$PEEA_{37}$ in Table 2). The monomer EEA was passed through of basic alumina to remove traces of residual acid. The PTHF macroinitiator (1.0 g, 0.19 mmol) was dissolved in the monomer EEA (4.1 mL, 0.028 mol), and the mixture was degassed by bubbling with N_2 for 1 h. Cu(I)Br (0.0271 g, 0.189 mmol) was added under a nitrogen atmosphere, and the reaction flask was immersed in a water bath thermostated at 50 °C. Polymerization was started by adding PMDETA (0.039 mL, 0.19 mmol). Samples were withdrawn periodically to monitor monomer conversion (by ^{1}H NMR) and molecular weight (by GPC). After termination in liquid nitrogen (150 min, 25% conversion), block copolymers were dissolved in THF and purified by elution through neutral alumina. Solvent was evaporated, and the residual monomer was removed under high vacuum.

^{1}H NMR ($CDCl_3$, 300 MHz) δ (ppm): 1.12 (s, 6H, $-C(CH_3)_2-$), 1.20−2.40 (broad, 13H, $-OCH_2CH_3$, $-COOCHCH_3-$, $-CH_2-$, $-CH-$ protons of PEEA and $-CH_2CH_2-$ protons of PTHF), 1.61 (broad, 4H, $-CH_2CH_2-$ protons of PTHF), 3.40 (4H, $-OCH_2-$ protons of PTHF), 3.40−3.80 (broad, 2H, $-OCH_2CH_3$ of PEEA), 5.86 (broad, 1H, $-COOCHCH_3$ of PEEA), 3.95 (d of t, 2H, $CH_2=CHCH_2-$), 3.97 (m, 3H, R_2CHBr and $-CH_2OC(=O)-$), 5.16 and 5.28 (d of quartets, 2H, $CH_2=CH-$), 5.91 (m, 1H, $CH_2=CH-$).

FT-IR (KBr, THF, neat) ν (cm^{-1}): 2940 (s), 2856 (s), 1724 (C=O, ester), 1447 (m), 1366 (m), 1241 (m) and 1210 (m) and 1164 (m) (acetal), 1110 (s), 799 (w).

Chain Extension of PTHF-*b*-PtBA-Br by ATRP of Styrene. A typical experiment was conducted as follows ($PTHF_{68}$-*b*-$PtBA_{12}$-*b*-PS_{64} in Table 3): PTHF-*b*-PtBA-Br macroinitiator (0.115 g, 0.0174 mmol), styrene (1.0 mL, 8.7 mmol), and PMDETA (0.0036 mL, 0.017 mmol) were mixed in a flask, degassed by three freeze−pump−thaw cycles, and kept under nitrogen. CuBr (0.0025 g; 0.017 mmol) was added to the frozen reaction mixture under nitrogen; the flask was closed, evacuated by three nitrogen/vacuum cycles, and heated in an oil bath at 110 °C. After 340 min (18% conversion), polymerization was terminated by cooling in liquid nitrogen. A solution of the polymerization product in THF was passed through neutral alumina in order to remove Cu. The triblock copolymer was precipitated in MeOH and dried under vacuum. GPC proved that clean block copolymerization was achieved, without any remaining macroinitiator (Figure 5b,c).

$M_{n,GPC}$ = 20 000 g/mol and M_w/M_n = 1.12 ($CHCl_3$ as solvent, PS standards); $M_{n,NMR}$ = 13 300 g/mol; 43/19/38 mol % PTHF/PtBA/PS.

^{1}H NMR ($CDCl_3$, 300 MHz) δ (ppm): 1.13 (s, 6H, $-C(CH_3)_2-$), 1.28−2.00 (broad, 18 H, $-CH_2CH_2-$ protons of PTHF, $CH_2/C(CH_3)_3-$ protons of PtBA and $CH_2/CH-$ protons of PS), 2.22 (s, 1H, C*H*− protons of PtBA), 3.41 (4H, $-OCH_2-$ protons of PTHF), 3.97 (d of t, 2H, $CH_2=CHCH_2-$), 4.05 (t, 2H, $-CH_2OC=O-$), 5.18 and 5.29 (d of q, 2H, $CH_2=CH-$), 5.88 (m, 1H, $CH_2=CH-$), 6.24−7.24 (broad, 5H, phenyl protons of PS).

FT-IR (KBr, CH_2Cl_2) ν (cm^{-1}): 3082−2731 (s), 1942, 1875, and 1803 (w) (overtones aromate), 1728 (s) (C=O, ester), 1688 (w), 1601 (m), 1583 (w), 1493 and 1453 (s) (C−C aromatic stretch), 1367 (m), 1249 (w), 1209 (w), 1149 (m), 1112 (s), 1029 (w), 908 (w), 846 (w), 758 (m), and 700 (s).

Hydrolysis of PTHF-*b*-PtBA. 2.28 g of $PTHF_{68}$-*b*-$PtBA_{224}$ with 85 wt % PtBA (Table 2) was hydrolyzed in 25 mL of CH_2Cl_2 at room temperature for 24 h with a 5-fold excess of trifluoroacetic acid with respect to the *tert*-butyl ester groups (5.61 mL, 75.6 mmol).[5] After the solvent evaporation, the copolymer was dissolved in THF and precipitated in pentane. Full conversion of PtBA to PAA was obtained, as confirmed by ^{1}H NMR and FT-IR data.

To be able to measure the PTHF-*b*-PAA block copolymers on GPC without problems of absorption of the hydrolyzed polymer on the column, the PAA block in PTHF-*b*-PAA was methylated with a (trimethylsilyl)diazomethane solution.[43] After methylation, PTHF-*b*-poly(methyl acrylate) is obtained, which does not interact with the GPC column and gives reliable GPC results when $CHCl_3$ is used as a solvent with polystyrene standards. $M_{n,GPC}$(PTHF-*b*-PMA) = 35 100 g/mol and M_w/M_n = 1.37 ($CHCl_3$ as solvent, PS standards).

^{1}H NMR (CD_3OD, 300 MHz) δ (ppm): 1.14 (d, 6H, $-C(CH_3)_3$, 1.25−2.00 (broad, 6H, CH_2 of PAA and $-CH_2CH_2-$ of PTHF), 2.42 (s, 1H, C*H* of PAA), 3.42 (4H, $-OCH_2-$ protons of PTHF), 3.95 (d of t, 2H, $CH_2=CHCH_2-$), 4.04 (t, 2H, $-CH_2OC(=O)-$), 4.28 (s, 1H, R_2CHBr), 5.13 and 5.26 (d of q, 2H, $CH_2=CH-$), 5.90 (m, 1H, $CH_2=CH-$).

FT-IR (KBr pellet pressed) ν (cm^{-1}): 3500−2340 (broad) (complexed COOH), 1764 (m), 1718 (vs) (complexed COOH), 1451, 1420, and 1364 (w), 1245 (m), 1170 (m), 1114 (m) (ν_{as} C−O−C), 812 (w)

Thermolysis of PTHF-*b*-PEEA. For thermolysis of the PTHF-*b*-PEEA block copolymers, the sample (typically 0.5 g) was spread out on a glass surface, which was heated in an oved at 80 °C for 48 h. Full conversion of PEEA to PAA was achieved, as proved by ^{1}H NMR and FT-IR data. For that reason, the corresponding spectra are the same as the ones described in the previous paragraph for the hydrolysis procedure.

Characterization. ^{1}H NMR spectra were recorded in $CDCl_3$ at room temperature, with a Bruker AM500 or a Bruker Avance 300 spectrometer. GPC was performed on a Waters instrument, using a refractive index detector (2410 Waters), equipped with Waters Styragel $10^3-10^4-10^5$ Å serial columns (5 μm particle size) at 35 °C. PS standards were used for calibration and $CHCl_3$ as eluent at a flow rate of 1.5 mL/min.

FT-IR spectra were recorded on a Perkin-Elmer 1600 series infrared spectrophotometer. KBr pellets were pressed after mixing and grinding the sample powder with dry KBr. For complexation studies, the samples were first dissolved in a buffer at the desired pH and then freeze-dried before analysis.

Thermogravimetric analysis (TGA) was performed with a PL-TGA (type PL-TG 1000, Polymer Laboratories) under nitrogen at a heating rate of 10 °C min^{-1} from 25 to 800 °C. A Perkin-Elmer DSC7 apparatus equipped with the thermal analysis controller TAC7/DX was used for differential scanning calorimetry (DSC) analysis. After a first heating and cooling cycle, the samples were heated from −110 to 70 °C at a scanning rate of 10 °C/min. Indium and octane were used for temperature calibration. Indium was also used for enthalpy calibration. The melting temperature (T_m) was evaluated from the onset of the baseline change for the endothermic signal, while the glass transition temperature (T_g) of each polymer was determined as the temperature at the midpoint of the transition.

Matrix-assisted laser desorption/ionization time-of-flight (MALDI-TOF) mass spectra were recorded on an Applied Biosystems Voyager DE STR MALDI-TOF spectrometer equipped with 2 m linear and 3 m reflector flight tubes and a 337 nm nitrogen laser (3 ns pulse). All mass spectra were obtained with an accelerating potential of 20 kV in positive ion mode and in linear and/or reflector mode. Dithranol (20 mg/mL in THF) was used as a matrix, LiCl (5 mg/mL) was used as a cationating agent, and polymer samples were dissolved in THF (1 mg/mL). A poly(ethylene oxide) standard with M_n equal to 4120 g/mol was used for calibration. All data were processed using the Data Explorer (Applied Biosystems) and Polymerix (Sierra Analytics) software package.

Dynamic Light Scattering (DLS). DLS measurements were performed on a Brookhaven Instruments Corp. BI-200 apparatus equipped with a BI-2030 digital correlator and an Ion Laser Technology argon laser (10 mW) at a wavelength of 488 nm. A refractive index matching bath of filtered decalin surrounded the scattering cell, and the temperature was controlled at 25 °C. The data were analyzed by the CONTIN algorithm, while the hydrodynamic diameter (D_h) and size polydispersity of the micelles were obtained by a cumulant analysis of the experimental correlation function. 0.1 wt % (1 g/L) solution of each polymer was prepared by direct dissolution into water buffered at the desired pH. Buffers and all the sample solutions were filtered through 0.45 μm syringe filters, except for samples at pH 3.

Potentiometric Titration. Potentiometric titration was performed with a Sartorius Professional PP-20 pH meter equipped with a glass electrode. The system was calibrated with buffer solutions of pH 4, 7, and 10. A 20 mL 0.1 M NaOH solution of polymer (0.1 g/20 mL) was titrated under continuous stirring with a 0.1 M HCl solution at room temperature. The solution was equilibrated until constant pH value.

Results and Discussion

A. Synthetical Strategy. 1. Preparation of PTHF-*b*-PtBA and PTHF-*b*-PEEA with a Dual Initiator. The general strategy for the preparation of PTHF and PtBA (or PEEA) containing block copolymers by the dual initiator strategy is outlined in Scheme 1. The dual initiator contains a primary alcohol, which is used as the initiating center for CROP of THF, as well an activated bromide, which is an efficient initiator for ATRP. Block copolymers were synthesized in two consecutive steps. First, well-defined bromoisobutyrate-terminated PTHF macroinitiators were prepared by CROP from the dual initiator. In a next step, the Br-functionalized macroinitiator was used for the initiation of the second block by ATRP. It was previously shown that the reverse route, starting with a macroinitiator prepared

Table 1. Synthesis of Well-Defined Br-Terminated Poly(tetrahydrofuran) (PTHF) Macroinitiators by Cationic Ring-Opening Polymerization with a Dual Initiator

code	time (min)	% conv[c]	$M_{n,NMR}$[d] (g mol^{-1})	$M_{n,MALDI-TOF}$[e] (g mol^{-1})	$M_{n,GPC}$[f] (g mol^{-1})	M_w/M_n[f]
$PTHF_{42}$[b]	8	10	3500	3350	7400	1.11
$PTHF_{68}$[b]	21	15	5300	5300	11200	1.21

[a] M_n = number-average molecular weight; M_w = weight-average molecular weight; M_w/M_n = polydispersity index; MALDI-TOF = matrix-assisted laser desorption/ionization time-of-flight; GPC = gel permeation chromatography; subscripts represent the degree of polymerization (DP). [b] 2,6-Di-*tert*-butylpyridine/trifluoromethanesulfonic anhydride/4-hydroxybutyl-2-bromoisobutyrate/tetrahydrofuran/allyl alcohol/2,2,6,6-tetramethylpiperidine = 1.5/1/1/166/4/4 at 25 °C. [c] Calculated by ^{1}H NMR. [d] M_n calculated by ^{1}H NMR: $M_{n,NMR} = [(I_{3.41}/4)/(I_{4.18}/2)] \times MW(THF) + MW(HBBIB)$, where $I_{3.41}$ and $I_{4.18}$ represent the peak intensities from PTHF (3.41 ppm) and from the end group at 4.18 ppm, respectively, and MW stands for the molar weight. [e] M_n determined by MALDI-TOF in linear mode, with dithranol as matrix and LiCl as cation. [f] M_n and M_w/M_n determined by GPC with $CHCl_3$ as eluent and calibrated with PS standards.

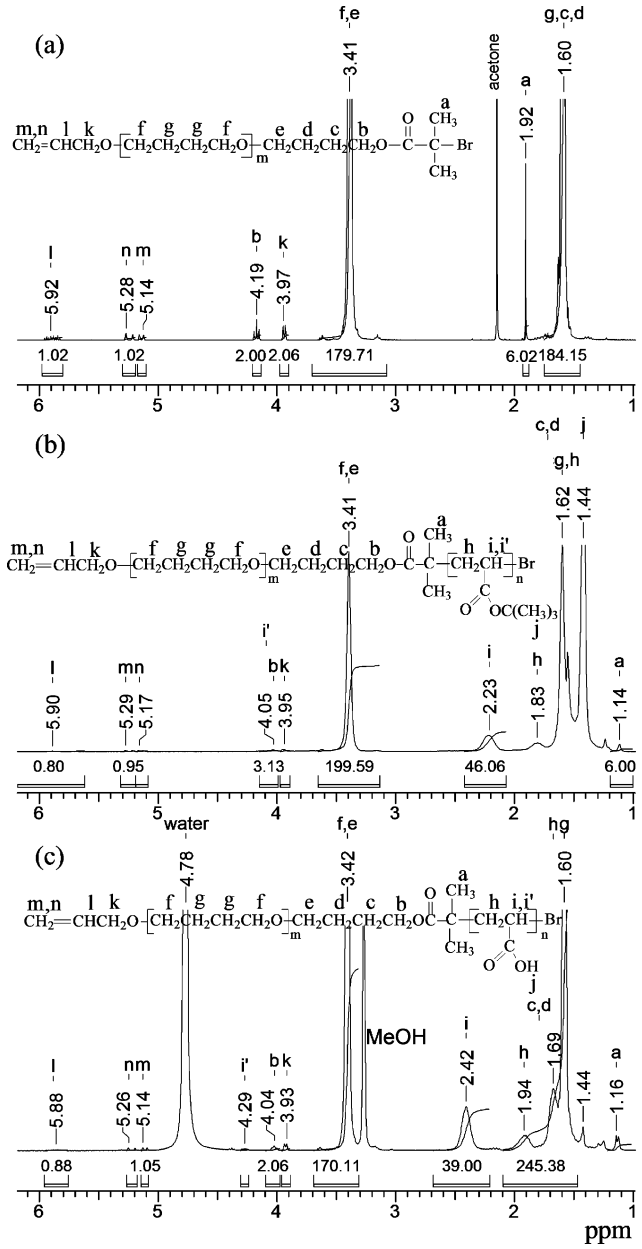

Figure 1. ^{1}H NMR spectra of (a) $PTHF_{42}$ macroinitiator ($CDCl_3$, 300 MHz, $d_1 = 30$ s), (b) $PTHF_{42}$-*b*-$PtBA_{20}$ before hydrolysis ($CDCl_3$, 300 MHz), and (c) $PTHF_{42}$-*b*-PAA_{20} after hydrolysis (CD_3OD, 300 MHz).

by ATRP and followed by CROP of THF, was less effective.[21] Polymerization of THF was initiated by HBBIB and terminated with allyl alcohol at room temperature to give well-defined living PTHF chains (see $PTHF_{42}$ and $PTHF_{68}$ in Table 1) functionalized at one end with the bromoisobutyrate group of the dual initiator and at the other end with an allyl group introduced by termination (reaction A in Scheme 1).

The end-group functionality of the PTHF macroinitiator was investigated by ^{1}H NMR and MALDI-TOF. Figure 1a represents the ^{1}H NMR spectrum of Br-functionalized PTHF. The 6/2 ratio of the integrations of the peaks of respectively $-C(CH_3)_2Br$ at 1.92 ppm and the methyl protons at 4.19 ppm proves that every PTHF chain contains a Br end group. The preservation of the Br functionality during CROP is crucial to obtain quantitative initiation for ATRP reactions with PTHF-Br as macroinitiator. The fine structure of the polymer was further confirmed by MALDI-TOF (Figure 2). Only one series of peaks, separated by 72 Da (THF repeating unit), can be detected. The good similarity in the shape and the mass values between the

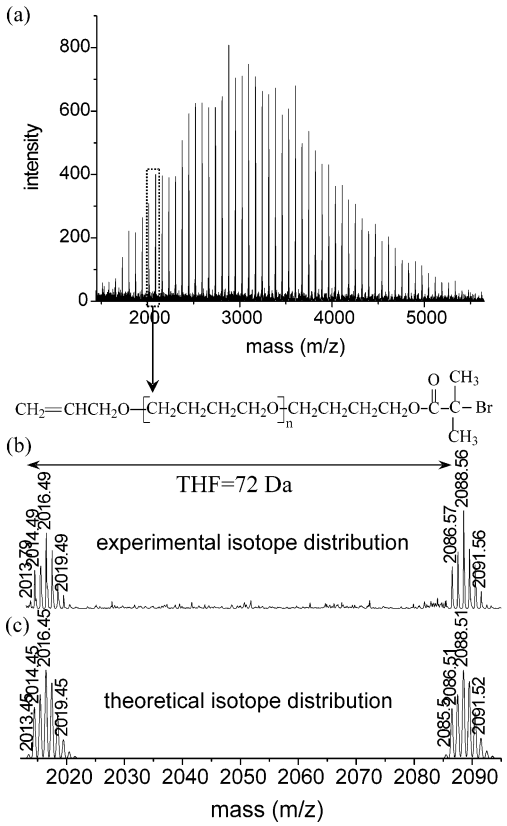

Figure 2. Reflectron mode MALDI-TOF spectrum of poly(tetrahydrofuran) ($PTHF_{42}$-Br in Table 1) with dithranol as matrix and LiCl as cation (a) full spectrum, (b) details of the experimental isotope distribution, and (c) details of the theoretical isotope distribution.

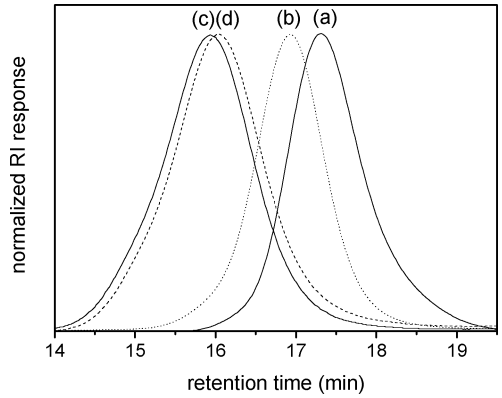

Figure 3. Gel permeation chromatography traces of (a) $PTHF_{68}$ macroinitiator (—), (b) $PTHF_{68}$-*b*-$PEEA_{37}$ (•••), (c) $PTHF_{68}$-*b*-$PtBA_{224}$ (—), and (d) $PTHF_{68}$-*b*-PMA_{224} (- - -).

experimental (Figure 2b) and the theoretical (Figure 2c) isotope distributions confirms that the PTHF macroinitiator is functionalized quantitatively and that side reactions could not be observed.

The Br-functionalized PTHF was used in a next step to initiate the ATRP of tBA in the presence of the CuBr/PMDETA complex as catalyst in acetone at 75 °C. A block copolymer PTHF-*b*-PtBA was formed, without the need for intermediate transformation or protection steps (pathway B in Scheme 1).

GPC profiles for the PTHF-Br macroinitiator and the resulting block copolymer are shown in Figure 3 (curves a and c). Upon copolymerization, the GPC curve of the macroinitiators was shifted to high molecular weight while a narrow molecular weight distribution was maintained. No GPC trace attributed to unreacted PTHF macroinitiator was observed. Figure 1

Table 2. Synthesis of Poly(tetrahydrofuran-*b*-*tert*-butyl acrylate) (PTHF-*b*-PtBA) or Poly(tetrahydrofuran-*b*-1-ethoxyethyl acrylate) (PTHF-*b*-PEEA) Block Copolymers by Atom Transfer Radical Polymerization of TBA or EEA Initiated by a PTHF-Br Macroinitiator

code[b]	$[M]_0:[I]_0$[c]	time (min)	% conv[d]	$M_{n,th}$[e] (g mol^{-1})	$M_{n,NMR}$[f] (g mol^{-1})	$M_{n,GPC}$[g] (g mol^{-1})	M_w/M_n[g]	PTHF/polyacrylate (mol %)[h]
$PTHF_{42}$-*b*-$PtBA_4$	150	6	5	4300	3800	7800	1.13	92/8
$PTHF_{42}$-*b*-$PtBA_5$	150	10	3	3800	3900	8100	1.13	90/10
$PTHF_{42}$-*b*-$PtBA_{26}$	150	15	22	7500	6600	10800	1.14	64/36
$PTHF_{42}$-*b*-$PtBA_{40}$	150	30	30	9200	8500	14150	1.22	52/48
$PTHF_{42}$-*b*-$PtBA_{68}$	150	39	39	10900	12000	14900	1.25	40/60
$PTHF_{42}$-*b*-$PtBA_{128}$	150	378	59	14700	19700	18800	1.19	26/74
$PTHF_{68}$-*b*-$PtBA_6$	150	20	9	7000	6100	14200	1.13	92/8
$PTHF_{68}$-*b*-$PtBA_{12}$	150	50	13	7845	6800	13800	1.15	86/14
$PTHF_{68}$-*b*-$PtBA_{17}$	300	60	5	7200	7400	1460	1.12	82/18
$PTHF_{68}$-*b*-$PtBA_{44}$	300	43.5	15	10900	10800	16900	1.12	62/38
$PTHF_{68}$-*b*-$PtBA_{79}$	300	109	26	15100	15300	19100	1.15	47/53
$PTHF_{68}$-*b*-$PtBA_{224}$	300	73	43	33000	33900	36000	1.35	24/76
$PTHF_{42}$-*b*-$PEEA_{37}$	50	120	74	8600	7700	11500	1.15	52/48
$PTHF_{68}$-*b*-$PEEA_{37}$	150	150	25	10700	10600	17400	1.12	66/34

[a] M_n = number-average molecular weight; M_w = weight-average molecular weight; M_w/M_n = polydispersity index; GPC = gel permeation chromatography; subscripts represent the degree of polymerization (DP). [b] $DP_{tBA} = [(I_{1.35-2} - I_{3.39})/11 \text{ or } I_{2.22}]/[I_{3.39}/4]) \times DP_{THF}$ and $DP_{EEA} = [(I_{3.1-3.9} - I_{1.6})/2]/[I_{1.6}/4] \times DP_{THF}$, where *I* represents the peak intensity for the protons with a chemical shift indicated by the subscript. [c] $[M]_0$ and $[I]_0$ are the initial concentration of monomer and initiator. Reaction conditions: [PTHF-Br macroinitiator]$_0$:[PMDETA]$_0$:[CuBr]$_0$ = 1:1:1 at 75 °C in acetone with tBA as monomer and [PTHF-Br macroinitiator]$_0$:[PMDETA]$_0$:[CuBr]$_0$ = 1:1:1 at 50 °C in bulk with EEA as monomer. [d] From ^{1}H NMR by comparison of a tBA monomer peak (δ = 6.3 ppm) with PTHF (δ = 3.41 ppm) as internal standard. In the case of EEA, an EEA monomer peak (δ = 6.4 ppm) and a PEEA peak (δ = 5.9 ppm) were used to calculate % conversion. [e] Theoretical M_n calculated as follows: $M_{n,th} = ([M]_0:[I]_0) \times MW_{acrylate} \times \%\text{ conversion} + M_n(\text{PTHF macroinitiator})$, where $MW_{acrylate}$ is the molecular weight of tBA or EEA and $[M]_0:[I]_0$ are the initial concentrations of the monomer and the macroinitiator, respectively. [f] $M_{n,NMR} = M_{n,NMR,polyacrylate} + M_n(\text{PTHF macroinitiator})$ with $M_{n,NMR,polyacrylate} = DP_{acrylate} \times MW_{acrylate}$. [g] GPC with $CHCl_3$ as solvent calibrated with PS standards. [h] Calculated by ^{1}H NMR from the integral values for PTHF (δ = 3.39 ppm) and PtBA (δ = 2.22 ppm) in the case of PTHF-*b*-PtBA. For PTHF-*b*-PEEA, the integral values for PTHF (δ = 1.6 ppm) and PEEA (δ = 1.1−1.4 ppm) were used.

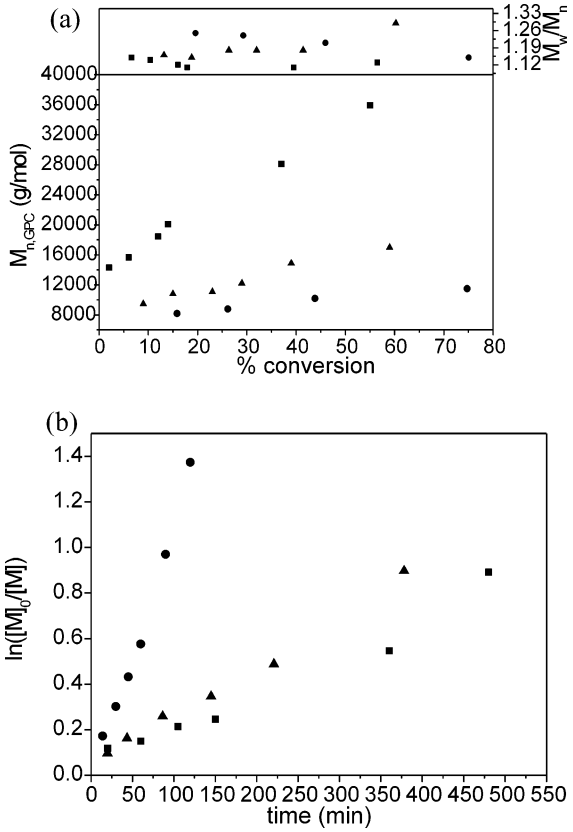

Figure 4. Kinetics for $PTHF_{42}$-*b*-$PtBA_{128}$ (▲), $PTHF_{68}$-*b*-$PtBA_{224}$ (■), and $PTHF_{68}$-*b*-$PEEA_{37}$ (●) from Table 1: (a) first-order kinetics and (b) evolution of $M_{n,GPC}$ (bottom) and M_w/M_n (top) with conversion.

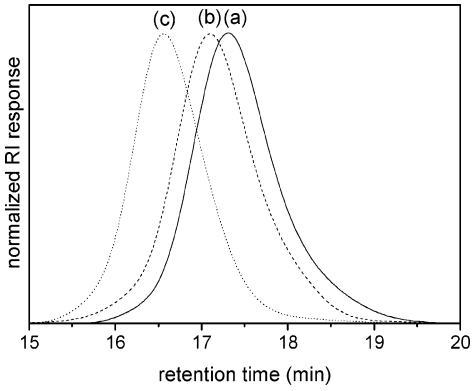

Figure 5. Gel permeation chromatography traces of (a) $PTHF_{68}$ (—), (b) $PTHF_{68}$-*b*-$PtBA_{12}$−Br (- - -), and (c) $PTHF_{68}$-*b*-$PtBA_{12}$-*b*-PS_{64} (•••).

illustrates the ^{1}H NMR spectra for PTHF-Br and a PTHF-*b*-PtBA copolymer. Attachment of PtBA to the PTHF macroinitiator was confirmed by the chemical shift of the methyl groups of the isobutyrate moiety, which changed from 1.92 ppm in PTHF-Br to 1.14 ppm upon block copolymerization, due to the replacement of the activated bromide by PtBA. Combination of GPC and NMR data leads to the conclusion that the initiation of ATRP of tBA by the PTHF macroinitiator is quantitative within the limits of sensitivity of these techniques.

Furthermore, the linear dependence of molecular weight on conversion and the linear relationship of $\ln([M]_0/[M])$ vs time (Figure 4a,b) support that ATRP of tBA is controlled when initiated by $PTHF_{42}$ and $PTHF_{68}$.

Table 2 summarizes the experimental conditions and molecular characteristics for the PTHF-*b*-PtBA copolymers. The experimental molecular weights, calculated by NMR, are in good accordance with the theoretical values. $M_{n,GPC}$ of the diblock copolymers is systematically higher than theoretical M_n, which is consistent with a polystyrene calibration. Polydispersity is lower than 1.35 (mostly lower than 1.25) for all copolymers.

As an alternative route to the use of tBA, another protected acrylic acid monomer, 1-ethoxyethyl acrylate (EEA),[23,42] was also polymerized successfully with PTHF-Br as a macroinitiator (entries named PTHF-*b*-PEEA in Table 2). The advantage of this route is that deprotection is easily carried out by thermolysis, with release of ethyl vinyl ether (boiling point: 33 °C), thus without the need of additional purification after deprotection. As shown by the kinetic results, the reaction proceeds in a controlled way (Figure 4). Well-defined block copolymers with

Table 3. Atom Transfer Radical Polymerization of Styrene Initiated by Br-Functionalized Poly(tetrahydrofuran-*b*-*tert*-butyl acrylate) (PTHF-*b*-PtBA-Br) as Macroinitiator ([CuBr]$_0$:[PMDETA]$_0$:[Macroinitiator]$_0$ = 1/1/1, 110 °C, Bulk)[a]

code	$[M]_0:[I]_0$	time (min)	% conv[b]	$M_{n,th}$[c] (g mol^{-1})	$M_{n,NMR}$[d] (g mol^{-1})	$M_{n,GPC}$[e] (g mol^{-1})	M_w/M_n[e]	PTHF/PtBA/PS (mol %)[f]
$PTHF_{68}$-*b*-$PtBA_6$-*b*-PS_{42}	300	400	16	11600	11000	16700	1.18	60/6/34
$PTHF_{68}$-*b*-$PtBA_{12}$-*b*-PS_{64}	500	340	18	16000	13300	20000	1.12	43/19/38
$PTHF_{68}$-*b*-$PtBA_{17}$-*b*-PS_{89}	500	75	20	17600	16700	20700	1.19	40/12/48

[a] M_n = number-average molecular weight; M_w = weight-average molecular weight; M_w/M_n = polydispersity index; GPC = gel permeation chromatography; PS = polystyrene; subscripts represent the degree of polymerization (DP). [b] % conversion was calculated from ^{1}H NMR by comparison of a styrene monomer peak (δ = 5.77 ppm) with PTHF (δ = 3.41 ppm) as internal standard. [c] Theoretical M_n calculated as follows: $M_{n,th} = ([M]_0:[I]_0) \times MW_{st} \times$ % conversion + M_n(PTHF-*b*-PtBA macroinitiator), where MW_{st} is the molecular weight of styrene and $[M]_0:[I]_0$ are the initial concentrations of the monomer and the macroinitiator, respectively. [d] $M_{n,NMR} = M_{n,NMR,PS} + M_n$(PTHF-*b*-PtBA macroinitiator) with $M_{n,NMR,PS} = DP_{st} \times MW_{st} = ([(I_{7.13} - I_{6.61})/5]/[I_{3.39}/4]) \times DP_{THF} \times MW_{st}$, where *I* represents the peak intensity for the protons with a chemical shift indicated by the subscript. [e] GPC with $CHCl_3$ as solvent calibrated with PS standards. [f] Calculated by ^{1}H NMR from the integral values for PTHF (δ = 3.39 ppm) and PtBA (δ = 1.35−2 ppm) and polystyrene (δ = 6.61−7.13 ppm).

Scheme 1. Reaction Scheme for the Synthesis of PTHF-*b*-PAA via the Dual Initiator Strategy

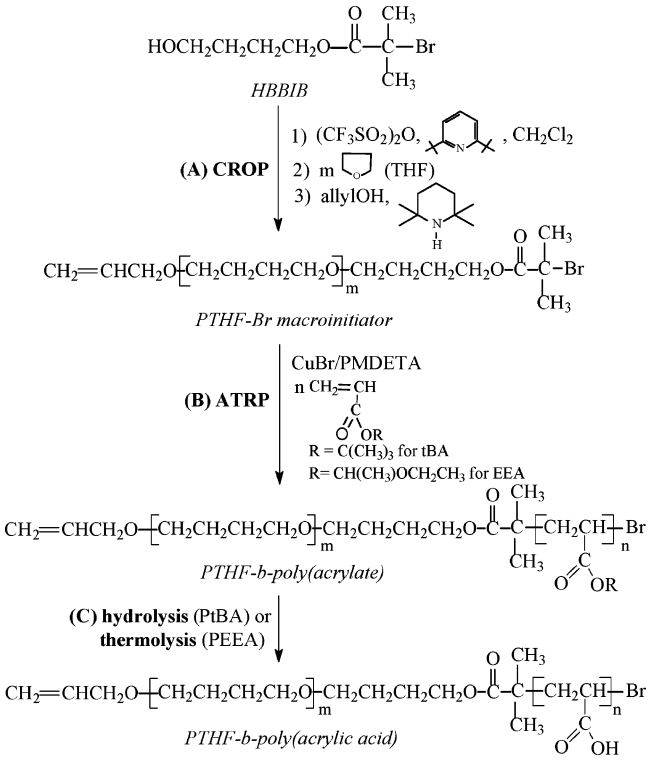

a low polydispersity were also prepared, and no residual macroinitiator was detected (Figure 3b).

2. Chain Extension Experiments. Livingness of the diblock copolymer chains was further proved by using them as macroinitiators for the ATRP of styrene catalyzed by the PMDETA/CuBr catalyst system at 110 °C. Extension of the AB diblock copolymers to ABC copolymers (Table 3) was assessed by clear shift of the GPC trace for the diblock copolymers toward higher molecular weight without visible trace of unreacted PTHF-*b*-PtBA-Br. The activated bromide was obviously preserved at the end of the diblock copolymers (Figure 5). Polydispersity was lower than 1.20 in all the cases.

3. Conversion of the Protected Blocks to PAA. *3.1. Hydrolysis of PtBA.* The *tert*-butyl ester groups of the PtBA blocks were cleaved by treatment with TFA in dichloromethane, which yields amphiphilic PTHF-*b*-PAA block copolymers at high pH. The hydrolysis can be followed by infrared analysis of the carboxylic acid groups that are formed (broad peak between 3500 and 2500 cm^{-1}) and the *tert*-butyl groups that disappear (asymmetric doublet at 1368 and 1389 cm^{-1}) (Figure 6). No signal is observed at 1.4 ppm in the ^{1}H NMR spectrum after hydrolysis which testifies to the complete hydrolysis of

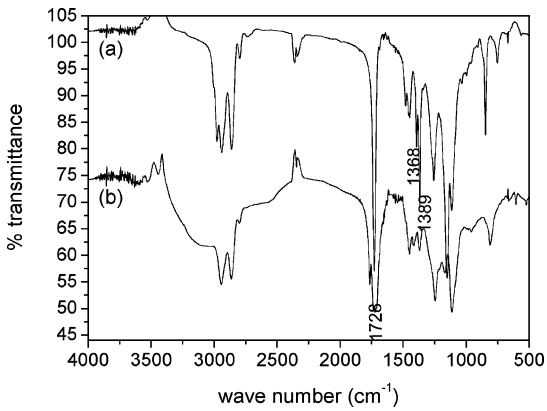

Figure 6. Fourier transform infrared spectra of (a) $PTHF_{68}$-*b*-$PtBA_{79}$ before hydrolysis and (b) $PTHF_{68}$-*b*-PAA_{79} after hydrolysis.

the *tert*-butyl ester groups of the PtBA blocks (Figure 1c). Moreover, PTHF is not degraded under the hydrolysis conditions as assessed by the ratio of $4H_f$ of PTHF (δ = 3.41 ppm) and $1H_i$ of PtBA or PAA that remains unchanged after hydrolysis.

To analyze the hydrolyzed block copolymers, PTHF-*b*-PAA, by GPC, methylation by a (trimethylsilyl)diazomethane solution[43] was carried out with formation of PTHF-*b*-poly(methyl acrylate) (PTHF-*b*-PMA) diblock copolymers. Figure 3d shows that methylation yields monomodal traces with low polydispersity, quite comparable to the values before hydrolysis. These observations demonstrate that the block copolymers survive the hydrolysis conditions and that the ester linkage between the two blocks remains intact under those circumstances. The slightly lower molecular weight of the methylated polymers compared to the PTHF-*b*-PtBA analogues can be attributed to the lower molar mass of MA compared to tBA.

3.2. Heating of PTHF-b-PEEA. As mentioned before, another route for the synthesis of PTHF-*b*-PAA consists of heating PTHF-*b*-PEEA. The NMR and FT-IR spectra are similar to those presented in Figures 1c and 6b. Thermogravimetric analysis of a purified sample of $PTHF_{68}$-*b*-$PEEA_{37}$ (Table 2) is shown in Figure 7. This block copolymer degrades at a lower temperature than $PTHF_{68}$-*b*-$PtBA_{224}$, which is consistent with thermolysis of PEEA and formation of PAA and volatile ethyl vinyl ether. Taking the molecular composition of $PTHF_{68}$-*b*-$PEEA_{37}$ into account, the theoretical weight loss is 24.1%. From TGA, an experimental weight loss of 23.0% (at 180 °C) is obtained, showing a good agreement between the theoretical and experimental value. PTHF-*b*-PEEA can be converted into PTHF-*b*-PAA without degradation of the PTHF-part.

B. Properties. 1. DSC of PTHF-*b*-PtBA. PTHF is a semicrystalline polymer with a T_g of −86 °C and a melting temperature in the 15−40 °C range, depending on the molecular

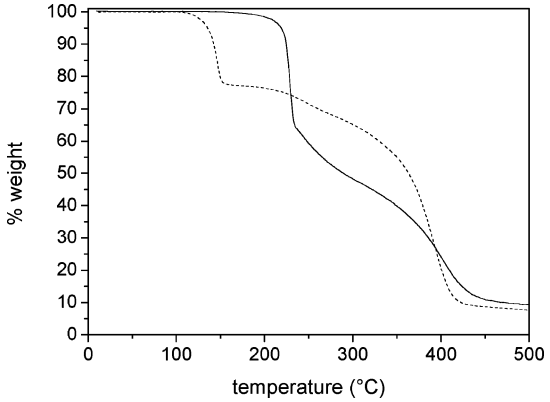

Figure 7. (a) Thermogravimetric analysis of $PTHF_{68}$-*b*-$PtBA_{224}$ (—) and $PTHF_{68}$-*b*-$PEEA_{37}$ (- - -) (heating rate 10 °C/min, N_2 atmosphere).

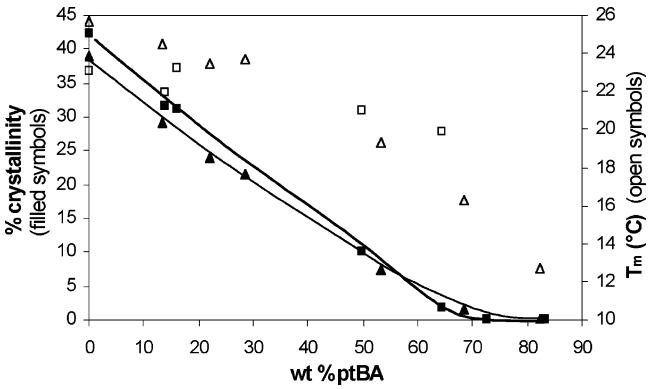

Figure 8. Differential scanning calorimetry study of the influence of PtBA incorporation on the crystallinity and melting point of $PTHF_{42}$ (■) or $PTHF_{68}$ (▲) (heating rate 10 °C/min) (filled symbols, % crystallinity; open symbols, T_m).

weight.[44] As both the degree of crystallinity and the melting temperature of the polymer determine the solid-state properties of the material, the influence of the incorporation of an amorphous PtBA block on the crystalline behavior of PTHF has been studied by DSC (Figure 8). The melting temperature of the homopolymer $PTHF_{68}$ (26 °C) is significantly decreased by increasing PtBA (amorphous) content. The relative crystallinity of the PTHF segments in the PTHF-*b*-PtBA block copolymers was calculated as follows:

$$\% \text{ crystallinity} = (m_{\text{PTHF}}/m_{\text{PTHF}-b-\text{PtBA}})(\Delta H_m/\Delta H_{m,100\%}) \quad (1)$$

with $\Delta H_{m,100\%} = 222$ J g^{-1},[45] m_{PTHF} the PTHF weight fraction in the block copolymer, and $m_{\text{PTHF}-b-\text{PtBA}}$ the total weight of the block copolymer sample used for DSC analysis.

The crystallinity decreases linearly with increasing PtBA content and disappears above 70 wt %. Those results clearly indicate that PtBA effectively disturbs the semicrystalline state of the PTHF domains.

The fact that the crystallinity of the $PTHF_{42}$ homopolymer is slightly higher than that of the $PTHF_{68}$ homopolymer[44] is also reflected in the crystallinity of the corresponding block copolymers up to a PtBA weight fraction of 0.58 (Figure 8). However, for high PtBA weight fractions, the copolymers with $PTHF_{42}$ segments show a lower crystallinity than that of the corresponding copolymers with $PTHF_{68}$ segments. Liu et al. published similar results for PTHF-*b*-PMMA.[46] By combination of small-angle X-ray scattering (SAXS), wide-angle X-ray diffraction (WAXD), and DSC data, they concluded that dispersed PTHF domains are formed at high content of the amorphous polymer.

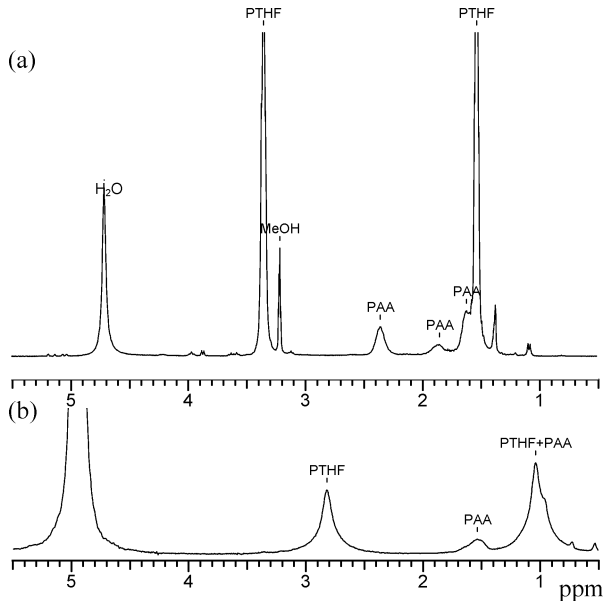

Figure 9. ^{1}H NMR spectra of $PTHF_{68}$-*b*-PAA_{44} in selective solvents: (a) CD_3OD common solvent and (b) 0.1 M NaOD pH 10 selective solvent for PAA (10 mg/0.7 mL solvent, 300 MHz).

The crystallizability of such domains increases with their size, thus for higher molecular weight of the PTHF segments.

2. pH-Responsive Properties. For the study of the pH-responsive properties, the following water-soluble block copolymers, obtained by hydrolysis of the PTHF-*b*-PtBA precursors in Table 2, were considered: $PTHF_{68}$-*b*-PAA_{44}, $PTHF_{68}$-*b*-PAA_{79}, and $PTHF_{68}$-*b*-PAA_{224}.

2.1. NMR in Selective Solvents. The hydrolyzed block copolymers are amphiphilic at high pH and expected to form micelles, as was reported for other polymers that were examined in different solvents by ^{1}H NMR spectroscopy.[47−49] Figure 9 shows the ^{1}H NMR spectra in MeOD (a good solvent for the two blocks) and in 0.1 M NaOD (a selective solvent for the PAA block).

The signal assigned to PTHF is decreased and broadened in NaOD (Figure 9b), whereas full signals characteristic of both the segments are detected in MeOD (Figure 9a). These results suggest that the hydrophobic PTHF block is surrounded by the hydrophilic PAA in NaOD (Figure 9a). Indeed, it is generally known that the polymer chains in the core of the micelles are less mobile and relatively dehydrated, which results in decreasing intensity and broadening of their NMR signals compared to chains located in the micelle corona.[50] This observation confirms the micellar behavior (Figure 10) of the hydrolyzed polymers and provides additional evidence that they are indeed block copolymers.

2.2. Complexation Study by FT-IR. The complexation behavior of $PTHF_{68}$-*b*-PAA_{74} at low (pH 3) and high pH (pH 10) was studied by FT-IR spectroscopy (Figure 11).

At low pH, the strong carboxyl absorption band around 1718 cm^{-1} and the broad band assigned to the OH absorption of carboxylic acid functions (3600−2300 cm^{-1}) indicate that the carboxyl groups are involved in H-bonding (Figure 11a). The hydrogen bonds can be intermicellar and lead to aggregates of micelles. The absorption should then be observed at 1703 cm^{-1}.[51] However, intramicellar hydrogen bonds can also be formed between the carboxyl groups of PAA and the oxygen groups of PTHF (Figure 10b), which accounts for a shift of the carbonyl absorption band of PAA to higher wavenumbers, as also observed by Cleveland et al.[52]

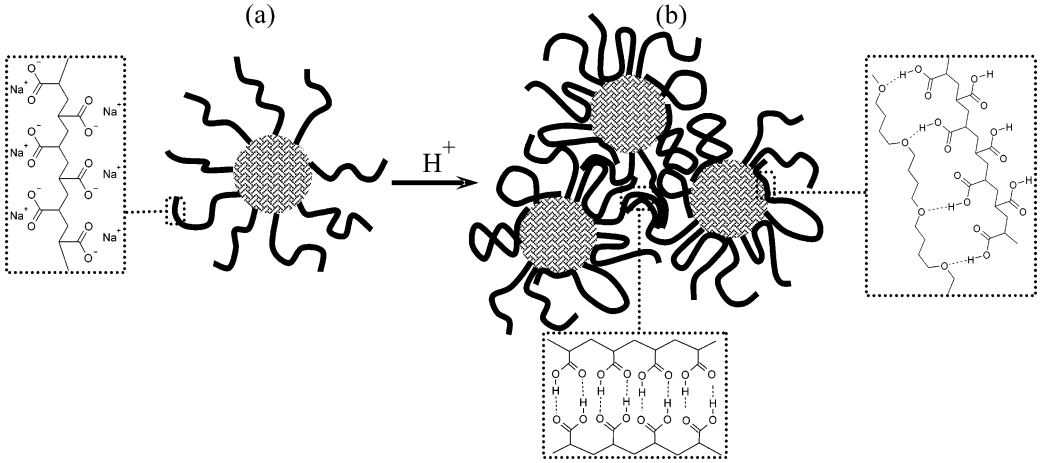

Figure 10. Schematic representation of structural transitions in PTHF-*b*-PAA induced by pH: (a) high pH, electrosterically stabilized micelles; (b) low pH, intermicellar H-bonding (bottom inset) and intramicellar attractive interactions (right inset) via protonated PAA chains (gray = PTHF, black = PAA).

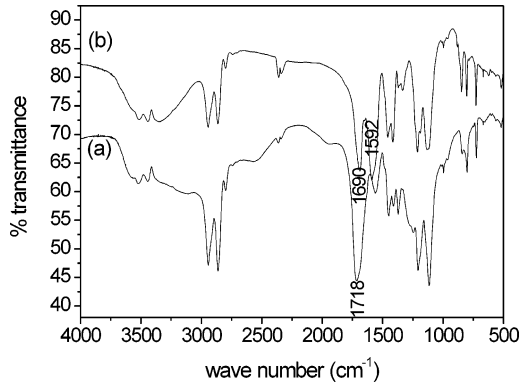

Figure 11. Fourier transform infrared spectra of $PTHF_{68}$-*b*-PAA_{79} (derived from $PTHF_{68}$-*b*-$PtBA_{79}$ in Table 2) at (a) pH 3 and (b) pH 10.

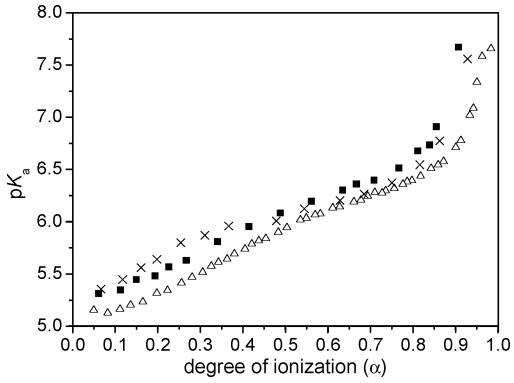

Figure 12. pK_a vs degree of ionization for $PTHF_{68}$-*b*-PAA_{44} (×), $PTHF_{68}$-*b*-PAA_{79} (■), and $PTHF_{68}$-*b*-PAA_{224} (△), obtained via back-titration.

Upon pH increase to pH 10, the OH absorption band becomes smaller (3600−3000 cm^{-1}) and a carboxylate peak (COO^-) becomes visible at 1690 and 1592 cm^{-1} (Figure 11b). Those results confirm the disappearance of intra- and intermolecular complex formation in basic medium.

2.3. Potentiometric Titration. The dissociation equilibrium of weak acidic polyelectrolytes such as PAA can be quantified by the apparent acid dissociation constant, K_a, which can be determined from the experimental pH and the degree of dissociation, α, by the Henderson−Hasselbach equation:

$$\mathrm{pH} = \mathrm{p}K_a - \log[(1 - \alpha)/\alpha] \qquad (2)$$

in which α is determined by the ratio of [PAA-COO^-]/([PAA-COO^-] + [PAA-COOH]).

The apparent pK_a values were determined for the different samples from the titration curves by plotting pH vs log[(1 − α/α)]. The higher the PTHF content of the block copolymer, the more the apparent pK_a diverges from the value for linear PAA homopolymers (p$K_{a,app}$ = 4.75[53]): p$K_{a,app}$($PTHF_{68}$-*b*-$PAA_{44/79}$) = 6.1 vs p$K_{a,app}$($PTHF_{68}$-*b*-PAA_{224}) = 5.9. As described earlier for copolymers of acrylic acid and *N*-dodecylmethacrylamide,[54] this increase in pK_a indicates that the acid−base equilibrium in hydrophobically modified poly(carboxylic acid)s is influenced by polymer bound hydrophobes in the vicinity of carboxyl groups.

In contrast to monomeric AA, for which a single pK_a of 4.26 can be calculated,[53] PAA shows a dependence of pK_a on α.[55,56] Therefore, in the case of the PTHF-*b*-PAA samples, pK_a was plotted as a function of the degree of ionization, α, calculated from eq 2 and the experimental pH determined from potentiometry (Figure 12). The pK_a value for PTHF-*b*-PAA increases with increasing α, which means that the amount of charged COO^- groups on the polymer chain increases and further dissociation becomes more difficult. Similar to PMAA-*b*-PMMA,[57] it is supposed that the PTHF-*b*-PAA copolymer forms a core−shell micelle at low pH, with a PTHF hydrophobic core consisting of aggregated PTHF segments and with a shell composed of PAA segments. Intermicellar hydrogen bonding is possible between COOH groups at the shells, while also intramicellar hydrogen bonding between PAA-COOH and PTHF takes place, as evidenced by FT-IR. With increasing α, the carboxylic acid groups of the shell are ionized and the shell layer is expanding, driven by the electrostatic repulsion between the negatively charged carboxylate groups. This is reflected by the plateau region in the middle of the pK_a vs α curves. However, electrostatic repulsion is not strong enough to overcome the hydrophobic attractive force of the PTHF core; thus, the conformation of the polymer and the micelle structure remains unchanged. The increase in the potentiometric titration curve beyond the plateau region indicates that further ionization is hindered by the electrostatic constraints imposed by the COO^- groups.[58]

2.4. Dynamic Light Scattering (DLS). Impact of pH on micellization and complex formation by PTHF-*b*-PAA has been studied by DLS. Copolymer solutions (0.1 wt %) were prepared in buffers at pH ranging from 3 to 10. As was also observed by Claverie et *al.*[38] for poly(*n*-butyl acrylate)-*b*-PAA, the largest particles are observed when the copolymers are fully protonated

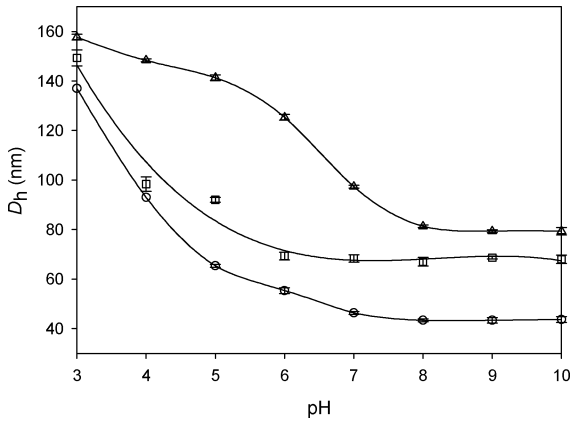

Figure 13. D_h vs pH for $PTHF_{68}$-*b*-PAA_{44} (○), $PTHF_{68}$-*b*-PAA_{79} (□), and $PTHF_{68}$-*b*-PAA_{224} (△), obtained by dynamic light scattering.

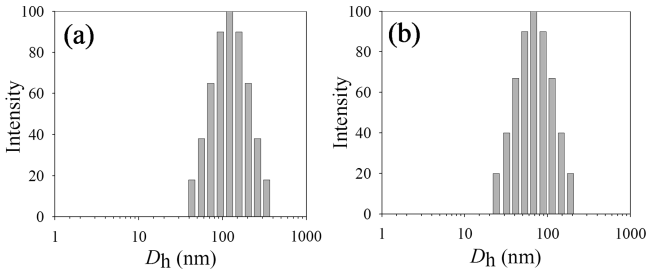

Figure 14. CONTIN size distributions for $PTHF_{68}$-*b*-PAA_{79} at (a) pH 3 and (b) pH 10.

(Figure 13). This is attributed to the formation of supermicellar aggregates (as proved earlier by FT-IR) due to absence of electrosteric stabilization, since PAA is uncharged (Figure 10b). It can also be noted that the micelles aggregation is more pronounced when the effective degree of ionization is very low, i.e., when pH is decreased below the apparent pK_a of the blocks (around 6, cf. titration results). Furthermore, a substantial increase in turbidity was also observed at low pH, in agreement with the formation of larger size scatterers. This was especially observed for the sample with the lowest PAA content, in which micelles are less stabilized ($PTHF_{68}$-*b*-PAA_{44}). Further increase in pH causes partial deprotonation, and electrostatic repulsion results in transition from micellar aggregates to individual micelles (Figure 10a), at pH close to apparent pK_a. This is confirmed by a decrease of the size of the objects to a minimum around the pK_a, D_h remaining constant at still higher pH. Previous FT-IR and NMR data indicated that micelles were formed at high pH, except for the sample with the higher PAA content ($PTHF_{68}$-*b*-PAA_{224}). An explanation might be that in the bulk copolymer chains are entangled and complexed by H-bonding (cf. FT-IR data in Figure 6b) and that this situation persists in acidic solution, with formation of larger objects. This effect should be more pronounced as the molecular weight of PAA is higher, as observed for $PTHF_{68}$-*b*-PAA_{224}. Since basic water is a better solvent for PAA and suppresses H-bonds, chain disentanglement could occur and individual core−shell micelles would be released (cf. NMR results in Figure 9b), accounting for a smaller diameter than at low pH.

The size of the micelles is directly related to the molecular weight of the PAA block and lies in the 40−80 nm range. The size distribution histograms for the aggregates and micelles were determined with the CONTIN routine. The representative CONTIN size distributions for the $PTHF_{68}$-*b*-PAA_{79} block copolymer at pH 3 and pH 10 are shown in Figure 14. Distributions are monomodal, and size polydispersity is typical of well-defined objects, i.e., lower than 0.2.

Conclusions

Well-defined PTHF-*b*-polyacrylate block copolymers with narrow polydispersity have been synthesized by ATRP of tBA (or EEA) initiated by PTHF-Br macroinitiators prepared by the dual initiator strategy. These block copolymers are viable precursors for pH-responsive PTHF-*b*-PAA copolymers. Crystallinity and melting temperature of semicrystalline PTHF are decreased in PTHF-*b*-PtBA copolymers as a result of the covalent bonding to PtBA.

For the PTHF-*b*-PAA block copolymers, a combination of ^{1}H NMR, FT-IR, potentiometric titration, and DLS emphasized that a transition from micellar aggregates to micelles upon increase in pH.

Acknowledgment. K. Bernaerts thanks the FWO (Fund for scientific research-Flanders, Belgium) for a PhD fellowship. The authors are indebted to the Belgian Science Policy in the frame of the Interuniversity Attraction Poles Program (PAI V/03). W. Van Camp thanks the IWT (The Institute for the Promotion of Innovation through Science and Technology in Flanders) for a PhD scholarship.

References and Notes

(1) Verdonck, B.; Goethals, E. J.; Du Prez, F. E. *Macromol. Chem. Phys.* **2003**, *204*, 2090−2098.
(2) Gohy, J.-F.; Willet, N.; Varshney, S.; Zhang, J.-X.; Jérôme, R. *Angew. Chem., Int. Ed.* **2001**, *40*, 3214−3216.
(3) Haulbrook, W. R.; Feerer, J. L.; Hatton, T. A.; Tester, J. W. *Environ. Sci. Technol.* **1993**, *27*, 2783−2788.
(4) Karymov, M. A.; Prochazka, K.; Mendenhall, J. M.; Martin, T. J.; Munk, P.; Webber, S. E. *Langmuir* **1996**, *12*, 4748−4753.
(5) Burguière, C.; Pascual, S.; Bui, C.; Vairon, J.-P.; Charleux, B.; Davis, K. A.; Matyjaszewski, K.; Bétremieux, I. *Macromolecules* **2001**, *34*, 4439−4450.
(6) Rösler, A.; Vandermeulen, G. W. M.; Klok, H.-A. *Adv. Drug Delivery Rev.* **2001**, *53*, 95−108.
(7) Vamvakaki, M.; Papoutsakis, L.; Katsamanis, V.; Afchoudia, T.; Fragouli, P. G.; Iatrou, H.; Hadjichristidis, N.; Armes, S. P.; Sidorov, S.; Zhirov, D.; Zhirov, V.; Kostylev, M.; Bronsteinfg, L. M.; Anastasiadis, S. H. *Faraday Discuss.* **2005**, *128*, 129−147.
(8) Verbrugghe, S.; Bernaerts, K.; Du Prez, F. E. *Macromol. Chem. Phys.* **2003**, *204*, 1217−1225.
(9) Schué, F. Comprehensive Polymer Science. In *Comprehensive Polymer Science*; Allen, G., Bevington, J. C., Eds. Pergamon: Oxford, 1989; Vol. 6, p 359.
(10) Kajiwara, A.; Matyjaszewski, K. *Macromolecules* **1998**, *31*, 3489−3493.
(11) Hawker, C. J.; Hedrick, J. L.; Malmström, E. E.; Trollsas, M.; Mecerreyes, D.; Moineau, G.; Dubois, P.; Jérôme, R. *Macromolecules* **1998**, *31*, 213−219.
(12) Mecerreyes, D.; Moineau, G.; Dubois, P.; Jérôme, R.; Hedrick, J. L.; Hawker, C. J.; Malmström, E. E.; Trollsås, M. *Angew. Chem., Int. Ed.* **1998**, *37*, 1274−1276.
(13) Merreceyes, D.; Atthoff, B.; Boduch, K. A.; Trollsås, M.; Hedrick, J. L. *Macromolecules* **1999**, *32*, 5175−5182.
(14) Puts, R. D.; Sogah, D. Y. *Macromolecules* **1997**, *30*, 7050−7055.
(15) Tao, L.; Luan, B.; Pan, C.-Y. *Polymer* **2003**, *44*, 1013−1020.
(16) Tunca, U.; Karhga, B.; Ertekin, S.; Ugur, A. L.; Sirkeciogiu, O.; Hizal, G. *Polymer* **2001**, *42*, 8489−8493.
(17) Tunca, U.; Erdogan, T.; Hizal, G. *J. Polym. Sci., Part A: Polym. Chem.* **2002**, *40*, 2025−2032.
(18) Weimer, M. W.; Scherman, O. A.; Sogah, D. Y. *Macromolecules* **1998**, *31*, 8425−8428.
(19) Xu, Y.; Pan, C.; Tao, L. *J. Polym. Sci., Part A: Polym. Chem.* **2000**, *38*, 436−443.
(20) de Geus, M.; Peeters, J.; Wolffs, M.; Hermans, T.; Palmans, A. R. A.; Koning, C. E.; Heise, A. *Macromolecules* **2005**, *38*, 4220−4225.
(21) Bernaerts, K. V.; Schacht, E. H.; Goethals, E. J.; Du Prez, F. E. *J. Polym. Sci., Part A: Polym. Chem.* **2003**, *41*, 3206−3217.
(22) Bernaerts, K. V.; Du Prez, F. E. *Polymer* **2005**, *46*, 8469−8482.
(23) Van Camp, W.; Du Prez, F. E.; Bon, S. A. F. *Macromolecules* **2004**, *37*, 6673−6675.
(24) Riess, G. *Prog. Polym. Sci.* **2003**, *28*, 1107−1170.

(25) Förster, S.; Abetz, V.; Müller, A. H. E. *Adv. Polym. Sci.* **2004**, *166*, 173-210.
(26) Ryan, A. J. *Faraday Discuss.* **2005**, *128*, 421−425.
(27) Eisenberg, A.; Rinaudo, M. *Polym. Bull. (Berlin)***1990**, *24*, (6), 671.
(28) Prochazka, K.; Kiserow, D.; Ramireddy, C.; Tuzar, Z.; Munk, P.; Webber, S. E. *Macromolecules* **1992**, *25*, 454−460.
(29) Kriz, T.; Masar, B.; Pospisil, H.; Plestil, J.; Tuzar, Z.; Kiselev, M. A. *Macromolecules* **1996**, *29*, 7853−7858.
(30) Stepanec, M.; Prochazka, K. *Langmuir* **1999**, *15*, 8800−8806.
(31) Stepanec, M.; Podhajecka, K.; Prochazka, K.; Teng, Y.; Webber, S. E. *Langmuir* **1999**, *15*, 4185−4193.
(32) Prochazka, K.; Martin, T. J.; Munk, P.; Webber, S. E. *Macromolecules* **1996**, *29*, 6518−6525.
(33) Ramireddy, C.; Tuzar, Z.; Prochazka, K.; Webber, S. E.; Munk, P. *Macromolecules* **1992**, *25*, 2541−2545.
(34) Yu, K.; Zhang, L.; Eisenberg, A. *Langmuir* **1996**, *12*, 5980−5984.
(35) Zhang, L.; Shen, H.; Eisenberg, A. *Macromolecules* **1997**, *30*, 1001−1011.
(36) Zhang, L.; Eisenberg, A. *Macromolecules* **1996**, *29*, 8805−8815.
(37) Zhang, L.; Eisenberg, A. *Science* **1995**, *268*, 1728−1731.
(38) Gaillard, N.; Guyot, A.; Claverie, J. *J. Polym. Sci., Part A: Polym. Chem.* **2003**, *41*, 684−698.
(39) Wang, C.; Ravi, P.; Tam, K. C.; Gan, L. H. *J. Phys. Chem. B* **2004**, *108*, 1621−1627.
(40) Feldthusen, J.; Ivan, B.; Müller, A. H. E. *Macromolecules* **1998**, *31*, 578−585.
(41) Schuch, H.; Klingler, J.; Rossmanith, P.; Frechen, T.; Gerst, M.; Feldthusen, J.; Müller, A. H. E. *Macromolecules* **2000**, *33*, 1734−1740.
(42) Hoogenboom, R.; Schubert, U. S.; Van Camp, W.; Du Prez, F. E. *Macromolecules* **2005**, *38*, 7653−7659.
(43) Couvreur, L.; Lefay, C.; Belleney, J.; Charleux, B.; Guerret, O.; Magnet, S. *Macromolecules* **2003**, *36*, 8260−8267.
(44) Dreyfuss, F. *Poly(tetrahydrofuran)*; Gordon and Breack Science: New York, 1982; Vol. 17.
(45) Wang, C.; Cooper, S. *Macromolecules* **1983**, *16*, 775−786.
(46) Liu, L.; Jiang, B.; Zhou, E. *Polymer* **1996**, *37*, 3937−3943.
(47) van Hest, J. C. M.; Delnoye, D. A. P.; Baars, M. W. P. L.; Genderen, M. H. P. v.; Meijer, E. W. *Science* **1995**, *268*, 1592−1595.
(48) Gitsov, I.; Fréchet, J. M. J. *J. Am. Chem. Soc.* **1996**, *118*, 3785−3786.
(49) Liu, S.; Armes, S. P. *Angew. Chem., Int. Ed.* **2002**, *41*, 1413−1416.
(50) Bütün, V.; Vamvakaki, M.; Billingham, N. C.; Armes, S. P. *Polymer* **2000**, *41*, 3173−3182.
(51) Chun, M.-K.; Cho, C.-S.; Choi, H.-K. *J. Appl. Polym. Sci.* **2004**, *94*, 2390−2394.
(52) Cleveland, C. S.; Guigley, K. S.; Painter, P. C.; Coleman, M. M. *Macromolecules* **2000**, *33*, 4278−4280.
(53) Glavis, F. J. Poly(Acrylic Acid) and its Homologs. In *Water Soluble Resins*; Davidson, R. L., Sittig, M., Eds.; Reinhold Book Corp.: New York, 1968.
(54) Sato, Y.; Hashidzume, A.; Morishima, Y. *Macromolecules* **2001**, *34*, 6121−6130.
(55) Kotin, L.; Nagasawa, M. *J. Chem. Phys.* **1962**, *36*, 873.
(56) Kawaguchi, Y.; Nagasawa, M. *J. Phys. Chem.* **1969**, *73*, 4382−4384.
(57) Ravi, P.; Wang, C.; Tam, K. C.; Gan, L. H. *Macromolecules* **2003**, *36*, 173−179.
(58) Monjol, P. *Bull. Soc. Chim. Fr.* **1972**, *4*, 1313−1318.

MA052625T